Bucher, Janina; Wurm, Thomas; Farshadfar, Kaveh; Schukin, Michael; Uzunidis, Georgios; Rudolph, Matthias; Rominger, Frank; Ariafard, Alireza; Hashmi, A. Stephen K.

Divergent Mechanistic Scenarios for the C−sp^2 and C−sp^3 C−H Insertion of Aurated Aryl Cations

Published in:
Advanced Synthesis and Catalysis

DOI:
10.1002/adsc.202300548

Published: 13/10/2023

Document Version
Publisher's PDF, also known as Version of record

Please cite the original version:
Bucher, J., Wurm, T., Farshadfar, K., Schukin, M., Uzunidis, G., Rudolph, M., Rominger, F., Ariafard, A., & Hashmi, A. S. K. (2023). Divergent Mechanistic Scenarios for the C−*sp*^{2} and C−*sp*^{3} C−H Insertion of Aurated Aryl Cations. *Advanced Synthesis and Catalysis*, *365*(19), 3320-3327. https://doi.org/10.1002/adsc.202300548

RESEARCH ARTICLE

doi.org/10.1002/adsc.202300548

Advanced Synthesis & Catalysis

Divergent Mechanistic Scenarios for the C–sp^2 and C–sp^3 C–H Insertion of Aurated Aryl Cations

Janina Bucher,[+a] Thomas Wurm,[+a] Kaveh Farshadfar,[b] Michael Schukin,[a] Georgios Uzunidis,[a] Matthias Rudolph,[a] Frank Rominger,[# a] Alireza Ariafard,[c, d] and A. Stephen K. Hashmi[a, e,]*

[a] Organisch-Chemisches Institut, Heidelberg University, Im Neuenheimer Feld 270, 69120 Heidelberg, Germany,
Fax: +49-6221-54-4205
E-mail: hashmi@hashmi.de
Homepage: http://www.hashmi.de

[b] Department of Chemistry and Material Science, School of Chemical Engineering, Aalto University, Kemistintie 1, 02150 Espoo, Finland

[c] School of Physical Sciences, University of Tasmania, Private Bag 75, Hobart TAS 7001, Australia

[d] Research School of Chemistry, The Australian National University, Canberra, ACT, Australia

[e] Chemistry Department, Faculty of Science, King Abdulaziz University (KAU), Jeddah 21589, Saudi-Arabia

[+] These authors contributed equally.

[#] Crystallographic investigation.

Manuscript received: May 25, 2023; Revised manuscript received: August 1, 2023;
Version of record online: August 23, 2023

Supporting information for this article is available on the WWW under https://doi.org/10.1002/adsc.202300548

Abstract: By employing the sterically highly demanding steering ligand IPr* at a gold(I) center, it is possible to induce a 6-*endo-dig* cyclization pathway in 1,5-diynes bearing terminal alkyne moieties. The resulting aurated naphthyl cations are utilized for the intermolecular formation of C–C bonds via C–H insertion of aromatic and aliphatic C–H bonds. The mechanisms of these transformations were studied by quantum chemical calculations.

Keywords: diynes; gold catalysis; aryl cations; C–H insertion; high energy intermediates

Introduction

In the recent past, the field of homogeneous gold catalysis[1] has seen the discovery of some remarkable high energy intermediates. By introducing the concept of dual activation,[2] Zhang *et al.*[3] and our group[4] independently demonstrated that diyne systems[5] can serve as precursors to diaurated gold vinylidene and diaurated aryl cation species.[6] For these transformations, two gold centers, which act synergistically to activate the diyne starting materials, are necessary. While one alkyne unit is rendered nucleophilic by the formation of a gold acetylide moiety,[7] the other alkyne unit is activated as an electrophile via the well-established π-coordination mode. Depending on their backbones, these dually activated diyne systems can cyclize either in a 5-*endo-dig* fashion, resulting in the formation of gold vinylidenes **II**,[8] or in a 6-*endo-dig* mode, leading to the formation of diaurated aryl cations of type **IV** (see Scheme 1).

Both intermediates were shown to be highly reactive and due to their ability to even insert into unactivated C(sp^2)–H as well as C(sp^3)–H bonds, a rich follow-up chemistry became accessible.[9]

By generalizing the concept of dual activation, we could demonstrate that high-energy intermediates can

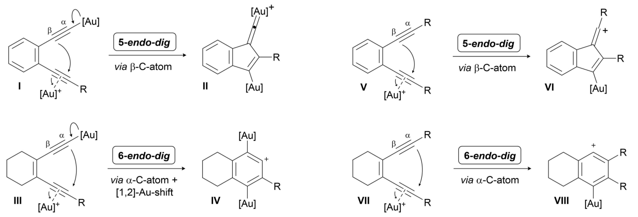

Scheme 1. Comparison of dual gold-catalyzed diyne cyclizations (left) with cyclizations initiated only by π-activation of one of the alkyne units (right).

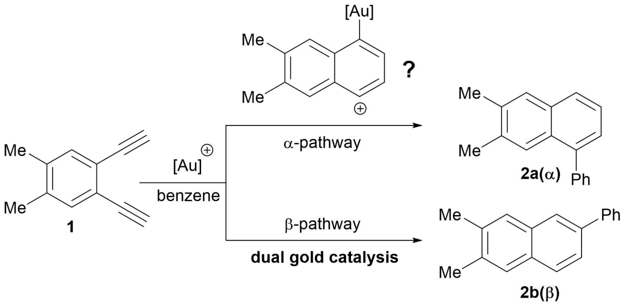

Scheme 2. Literature-known gold-catalyzed transformations of diyne **1**.

already be generated in the presence of only one gold center. In this context, we were first able to substitute the π-activated alkyne unit with suitable leaving groups as electrophiles. In these systems gold vinylidenes are formed when starting from gold acetylides alone and therefore new monoaurated vinylidene species are accessed.[7] Recently, we could show that related diyne starting materials can be cyclized after activation with only one gold catalyst, too. In these cases, the nucleophilic acetylide moiety is replaced by an internal alkyne unit and respective cyclizations are solely induced by π-activation of one of the alkyne units of the diyne system. By properly adjusting the substitution pattern of the diynes, we were able to realize the analogues of both cyclization modes known from dual gold-catalyzed transformations. Starting from alkynes with a phenylene linker, simple π-activation induced the 5-*endo*-*dig* pathway, leading to aurated vinyl cation intermediates **VI**.[10] On the contrary, employing vinylene-linked systems triggered the 6-*endo*-*dig* cyclization resulting in the formation of monoaurated phenyl cation species **VIII**.[11]

The so far obtained experimental data demonstrate that, under properly chosen reaction conditions, diyne systems in the presence of a cationic gold catalyst can serve as new and readily accessible precursors to these interesting high-energy intermediates, which so far have been synthesized from potentially toxic and hazardous precursors, e. g. diazo compounds.[12] Based on these now established mono gold reactivity pathways, so far only diyne systems with two internal alkyne units have been employed and the new intermediates have always been trapped *intra*molecularly. During our ongoing research program, we were curious whether diynes with two terminal alkyne moieties could serve as suitable precursors, too. In this case an *inter*molecular trapping of the intermediary generated species might become feasible. During our investigation on this reactivity pattern, we decided to reinvestigate the chemistry of diyne **1**. Our group has already demonstrated that conversion of **1** in presence of a gold catalyst in benzene as solvent delivers the corresponding α- and β-substituted naphthalene derivatives **2a(α)** and **2b(β)** (Scheme 2).[4] The pathway leading to the β-product (**2b(β)**) was the now well investigated foundation, leading to the field of dual gold catalysis. In contrary, no deeper studies on the formation of α-product **2a(α)** were conducted. Its structure of an α-naphthalene derivative however, together with experimental observations that it becomes the main product by using sub-stoichiometric amounts of gold catalyst, as well as in absence of basic additives, is consistent with a mechanism in which π-activation of one of the alkyne units leads to the formation of an aurated aryl cation **VIII**, which is subsequently trapped by benzene as solvent.

Following this hypothesis, we assumed that it should be possible to render the conversion of **1** fully α-selective, if it was possible to suppress formation of gold acetylides as well as *gem*-diaurated species, the key intermediates for the catalyst transfer mechanism of dual gold catalysis.[13]

Results and Discussion

We anticipated that this goal could be achieved by employing a gold catalyst with a sterically highly demanding steering ligand. Therefore, our choice fell on the IPr*-NHC ligand developed by Berthon-Gelloz and coworkers.[14] To our delight, when employing this catalyst system, the solely detectable reaction product was indeed **2a**, which, after a subsequently conducted full optimization of the reaction conditions (for further details see the supporting information) could preparatively (0.8 mmol) be isolated in 95% yield.

With these optimized reaction conditions in hand, we decided to evaluate the reaction scope of the applicable diyne systems, as well as the aromatic hydrocarbon nucleophiles (see Scheme 3). During the evaluation of the applicable diyne systems, it was possible to isolate the desired products, these originated from a diverse array of diynes with electronically modified benzene backbones. Depending on the exact nature of the substitution pattern, obtained yields varied from excellent 95% (**2a**), which were obtained for the model system and moderate yields of 50–40%

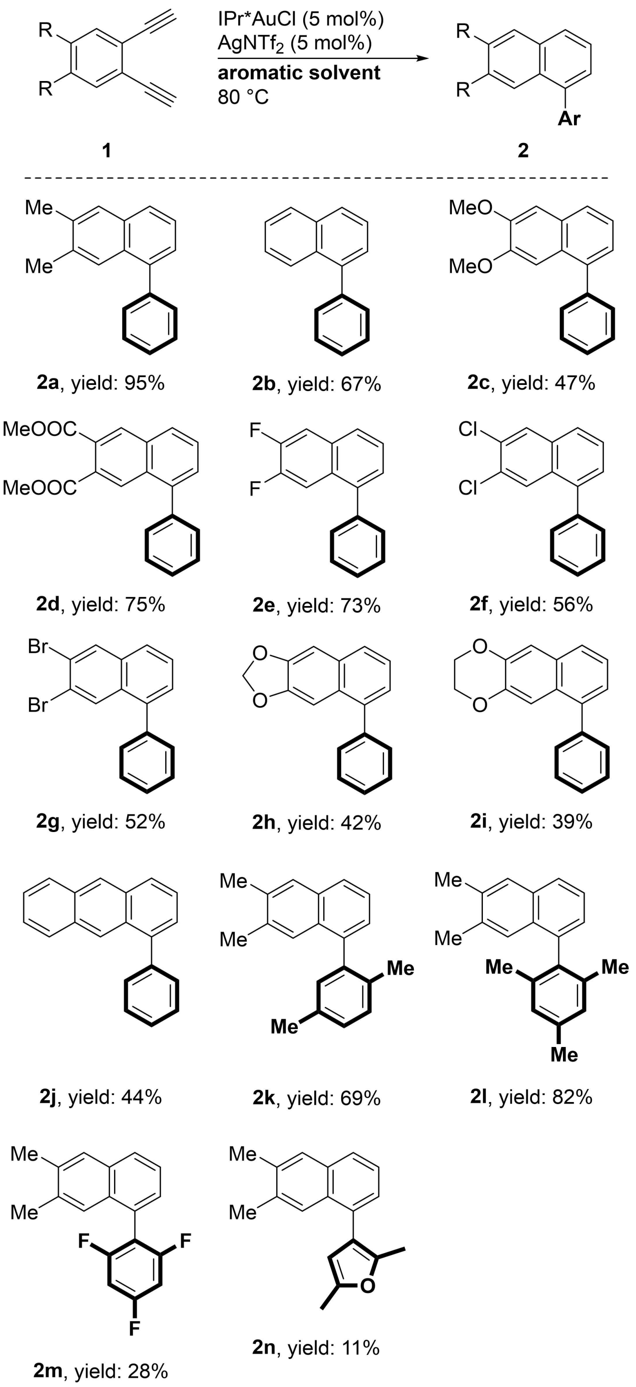

Scheme 3. Scope of the intermolecular aurated aryl cation mediated C–H insertion reaction with respect to the diyne and the aromatic hydrocarbon.

which were obtained for systems possessing especially electron-rich benzene backbones (**2c**, **2h**, **2i**). In addition to these substrates, it was possible to establish that diynes containing a naphthalene rather than a benzene backbone also follow this reactivity pattern (**2j**). Thereby the series of accessible aryl cations could be extended to the respective anthracenyl cation. After evaluation of the scope with respect to the diyne, the applicability of different aromatic nucleophiles was examined, too. It was observed that, apart from benzene, also *p*-xylene (**2k**) as well as mesitylene (**2l**) could be readily applied and the corresponding biphenyl derivatives were obtained in good yields of 69% and 82%. Further experiments to extend the reaction scope to 1,3,5-trifluorobenzene (**2m**) or the heterocyclic 2,5-dimethylfuran (**2n**) resulted only in the isolation of rather poor yields of the expected products.

Nevertheless, it is important to emphasize that, despite the presence of rather weak benzylic C–H bonds, experimentally only products resulting from the formal activation of a nominally stronger aromatic C–H bond were observed. Based on this experimental observation we conclude that the activation of aromatic C–H bonds in comparison to (so far only for intramolecular cases established)[11] aliphatic C–H bonds at the aryl cation center follow an entirely different mechanism which renders aromatic C–H bonds to be activated more facile. These differences will be explained in the theoretical part of this manuscript.

As a next step we were highly interested in the question if an *inter*molecular insertion into aliphatic C–H bonds is also possible with the developed synthetic regime. Related *intra*molecular C–H insertions were described for similar systems using platinum-, ruthenium-catalyzed[15] or gold-catalyzed transformations.[11] To investigate this possibility, we decided to vary our optimized reaction conditions for the formation of **2a** by replacing benzene for cyclohexane as solvent. By this procedure and under otherwise unchanged conditions, we were indeed able to isolate a novel compound **4a** in 66% (Scheme 4). A single crystal X-ray crystallographic investigation unambiguously established the constitution of **4a** as the expected respective α-selective cyclohexane C–H insertion product (see Figure 1).[16]

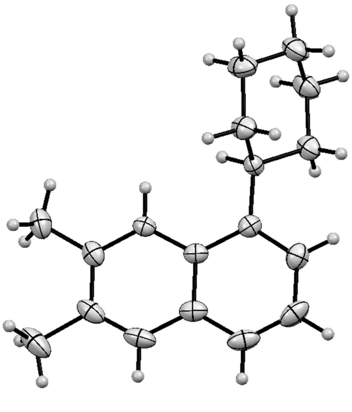

Figure 1. Solid state molecular structure of **4a**.

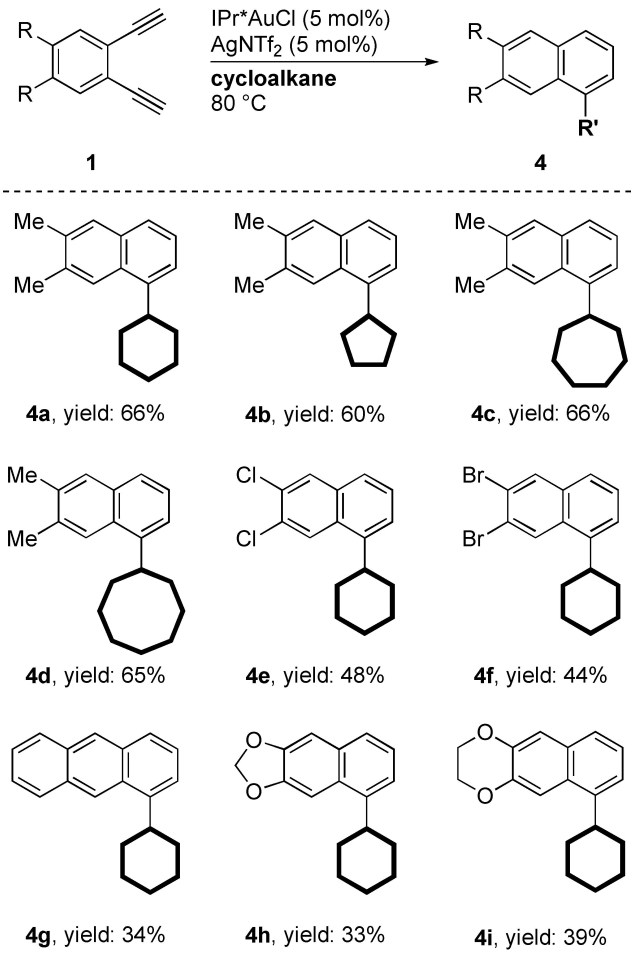

Scheme 4. Scope for the intermolecular aurated aryl cation mediated C–H insertion reaction with respect to the diyne and the aliphatic hydrocarbon.

Cyclopentane (**4b**), cycloheptane (**4c**) and cyclooctane (**4d**) were also suitable reactants, but the yields in a range of 60% to 66% remained lower than in the case of aromatic hydrocarbons, despite an undertaken optimization (Scheme 4). The trend of lower isolated yields for the C–H insertion at aliphatic hydrocarbons compared to aromatic hydrocarbons was also observed for other diynes. This experimental finding that aromatic hydrocarbons behave as better trapping reagents if compared to their aliphatic counterparts, again indicates that a different mechanism is in operation. The reduced yields for the aliphatic trapping case might be a result of an uncontrolled trapping of the reactive intermediate with unreacted (diyne) starting material or even already formed reaction products. As a next step, we evaluated the possibility to realize further site selectivity among aliphatic C–H bonds with varying bond strengths. To investigate this issue, we chose to utilize 2-ethylpentane as a solvent for our reaction (see Scheme 5), which possesses one tertiary C–H bond, six nominally stronger secondary C–H bonds and nine, even stronger, primary C–H bonds. During the experiment we expected, in analogy to the reaction of other highly electrophilic organometallic species e. g. Rh-carbene intermediates,[17] or the classical radical bromination reaction a preference for the weakest C–H bonds (tertiary followed by secondary C–H bonds), which should overrule the statistical factor (by weighing the occurrence of the respective bonds). However, experimentally an entirely different result was obtained. It was found, that the primary C–H bonds of 2-ethyl pentane (normalized to the number of CH bonds) react 1.6 times faster than the secondary C–H bonds, while the product, which would result from insertion into the tertiary C–H bond was not detected. We also performed deuterium labelling experiments in perdeuterated benzene and perdeuterated cyclohexane (Scheme 5b). In both cases we isolated the appropriate products. As expected, all remaining deuterium atoms of the incorporated deuterated solvent remained in the molecule. Furthermore, a selective deuterium incorporation into the C–H bonds of the newly formed ring systems was not observed. In both cases, all three positions were partly deuterium labeled. For the conversion in C_6D_6 an overall deuterium labeling of 0.5 was calculated, and for C_6D_{12} a similar result of 0.6 was observed. Furthermore, a competition reaction was conducted which showed that the insertion into benzene is favored over cyclohexane (Scheme 5c).

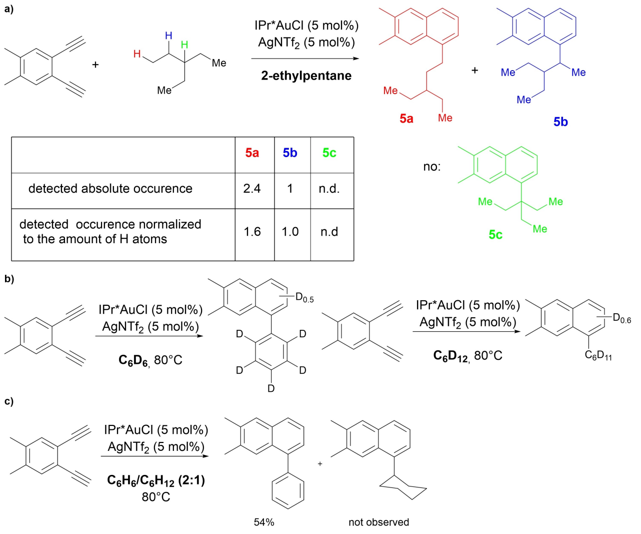

	5a	5b	5c
detected absolute occurence	2.4	1	n.d.
detected occurence normalized to the amount of H atoms	1.6	1.0	n.d

Scheme 5. Experiment to evaluate site selectivity in the intermolecular aurated aryl cation-mediated a) aliphatic C–H bond insertion reaction, b) deuterium labelling experiments, c) aromatic vs. aliphatic C–H activation experiments.

From this experimental observation it has to be concluded that, in analogy to the investigation of the intramolecular trapping of aurated phenyl cations,[11] the herein generated aurated naphthyl cations are highly reactive intermediates which are not suitable for positional-selective reactions. From the collected data it appears that the only factor determining the observed selectivity is the steric accessibility of the respective C–H bond.

Density functional theory (DFT) calculations were exploited to shed some light on the mechanism of the title reaction. Figure 2 shows the energy profile for the intermolecular insertion of a cyclohexane C(sp^3)–H bond into in-situ generated aurated naphthyl cation. Accordingly, the catalytic process is commenced by the ligand exchange between IPrAuNTf$_2$ and diyne **I**^{c} to give π-complex **II**^{c} in an endergonic fashion ($\Delta G^{\neq} = 11.0$ kcal/mol, Figure 2a). The higher stability of outer sphere complex **II**^{c} with respect to the infinitely separated ions **II'**^{c} and [NTf$_2$]$^-$ indicates the high importance of cation–anion interactions in these systems, mainly originated from low polarity of the solvent. Consistent with our previous DFT study,[11] intermediate **II**^{c} drives the 6-*endo-dig* cyclization via transition structure **TS**$_{\mathbf{II}}^{c}$ to give naphthyl cation **III**^{c} with a relative free energy of 22.7 kcal/mol.[18] The resultant intermediate then reacts with the solvent (cyclohexane) in a barrierless way and generates Wheland-type species **IV** with an exergonicity of −45.3 kcal/mol. The barrierless nature of the addition of the C(sp^3)–H bond to **III**^{c} is further confirmed by various relaxed Potential Energy Surface (PES) scans for reaction of methane and a model gold complex (Scheme S1). This computational result nicely connects to the above-discussed experimental result (Scheme 5), which have shown that the position selectivity in aliphatic hydrocarbon insertion is largely guided by the steric accessibility of the C–H bond rather than its bond strength.

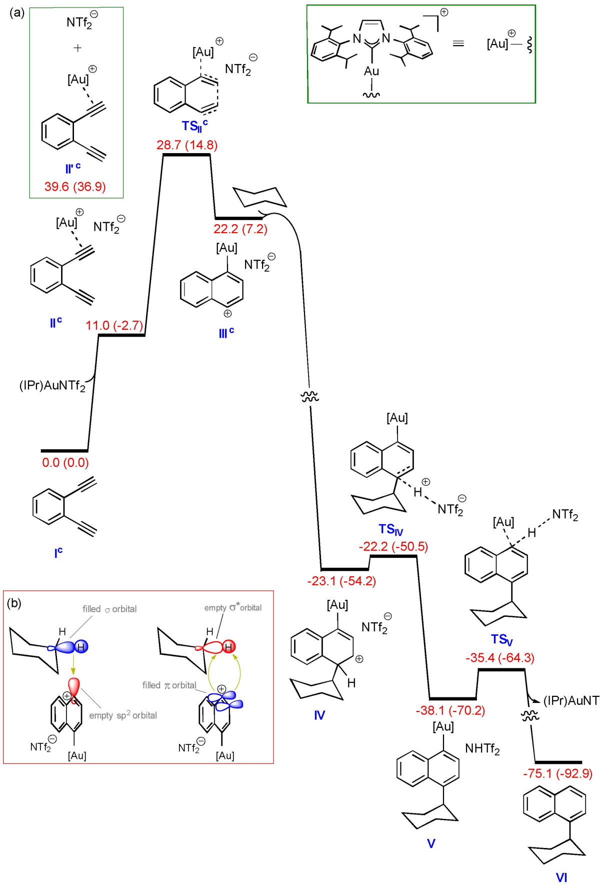

Figure 2. (a) Calculated energy profile for intermolecular insertion of a cyclohexane C(sp^3)–H bond into in-situ generated aurated naphthyl cation **III**^{c}. The relative Gibbs free energies and potential energies (in parenthesis) obtained from SMD/B3LYP-D3/def2-TZVP//SMD/B3LYP-D3/6-31G(d),SDD in cyclohexane are given in kcal/mol.(b) Schematic illustration of the orbitals involved in the formation of Wheland-type species **IV**.

Figure 2b shows orbital interactions between the cyclohexane C–H bond and the naphthyl cation C$_1$ atom. Accordingly, the filled σ-orbital of the C–H bond interacts with the empty sp^2 orbital of the C$_1$ atom. The strong nature of this interaction lowers the energy level of the σ*-orbital of the C–H bond, allowing it to interact easily with a filled π-orbital on the naphthyl cation and receive two electrons from it. These two interactions result in the naphthyl cation C$_1$ atom oxidatively inserting into a C–H bond of cyclohexane, giving Wheland-type species **IV**.

Once **IV** has formed, it is deprotonated by the [NTf$_2$]$^-$ counterion via transition structure **TS**$_{\mathbf{IV}}$, furnishing **V** from which a protodeauration occurs to afford product **VI** along the regeneration of the IPrAuNTf$_2$ catalyst by overcoming an energy barrier as low as 2.7 kcal/mol. The low barrier obtained for the protodeauration step is in line with the DFT results of previous studies.[19] Our computational results predict that the cyclization step with an overall activation free energy of 28.7 kcal/mol is the rate determining step. This relatively high barrier explains why the reaction experimentally needs an elevated temperature (80 °C) to operate.

Now, let us turn our attention to the mechanism of the benzene insertion at the aurated naphthyl cation as a model reaction for activation of aromatic C(sp^2)–H bonds (Figure 3a). Interestingly, in this case, as predicted by our DFT calculations, no Wheland-type species is formed during the catalytic process. We found that the addition of benzene to the aurated naphthyl cation **III**^{b} involves a barrierless path and, instead of formation of a Wheland-type intermediate, leads to phenonium ion **VII**. Again, similar to the aliphatic C–H insertion, a relaxed PES scan further confirms our claim that trapping of the benzene molecule by the aurated naphthyl cation directly affords the phenonium ion (SI, Scheme S2). Haberhauer and coworkers, also proposed a similar intermediate during the activation of benzene in a related

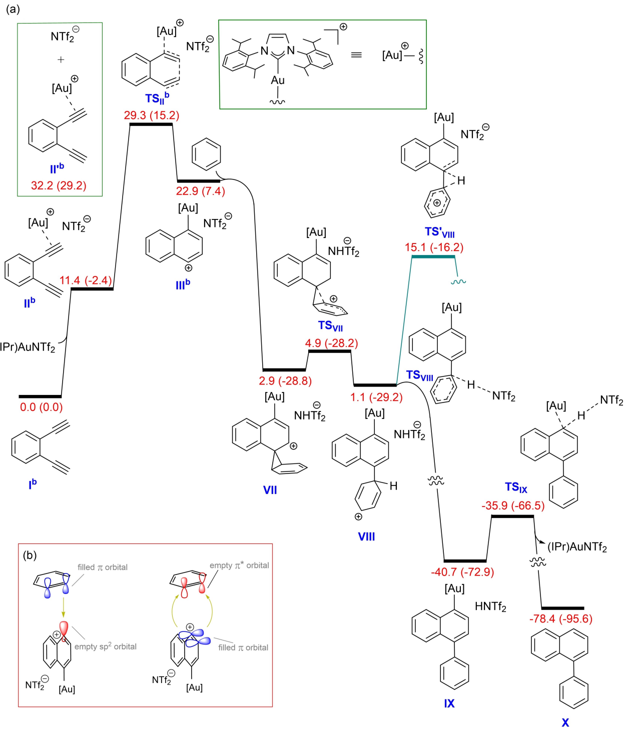

Figure 3. (a) Calculated energy profile for intermolecular insertion of a benzene C(sp^2)–H bond into in-situ generated aurated naphthyl cation **III^b**. The relative Gibbs free energies and potential energies (in parenthesis) obtained from SMD/B3LYP-D3/def2-TZVP//SMD/B3LYP-D3/6-31G(d),SDD in cyclohexane are given in kcal/mol. (b) Schematic illustration of the orbitals involved in the formation of the phenonium ion **VII**.

gold-catalyzed transformation.[20] The orbital interactions depicted in Figure 3b help in understanding how phenonium ion **VII** is formed. Accordingly, while the benzene binds to the C$_1$ atom of the naphthyl cation by σ-donating one of its π electrons, it receives the π electrons of the $C^1{=}C^2$ double bond via one of its π* orbitals. Since the π orbitals of benzene lie much higher in energy than its C–H σ-orbitals and its π* orbitals lie much lower in energy than its C–H σ*-orbitals, this aromatic substrate preferentially binds to the C^1 atom via its π system. Our calculations show that the phenonium ion **VII** is not reactive toward a desired chemical reaction and for it to become activated, it must isomerize to pentadienyl cation **VIII** in which the $C^1{=}C^2$ π-bond remains intact and the net positive charge is mainly localized on the C$^{4'}$ atom of the benzene. The ensuing intermediate **VIII** is a branching point for two pathways. It can either participate in the oxidative cleavage of the C–H bond via transition structure **TS′$_{\text{VIII}}$** to give Wheland-type intermediate **IX** or undergoes a deprotonation via transition structure **TS$_{\text{VIII}}$** to produce intermediate **X**. Due to the existence of the π system, the naphthyl cation C$_1$ atom is not capable of interacting effectively with one of the benzene C–H bonds, resulting in formation of the Wheland-type species for this substrate occurring with a higher activation barrier than that for cyclohexane. Alternatively, the presence of the [NTf$_2$]$^-$ anion around the coordination sphere of the gold cationic complex triggers the deprotonation reaction. The high acidity of the pentadienyl cation **VIII** renders the deprotonation by [NTf$_2$]$^-$ highly fast evident from our DFT result; **TS$_{\text{VIII}}$** is not identified as a saddle point because of the flatness of the PES near the transition state. As such, in contrast to the catalytic process involving insertion of the C(sp^3)–H bonds, that for the C(sp^2)–H bonds most likely proceed via a mechanism in which the Wheland-type species does not correspond to a key intermediate, supported by the result that **TS$_{\text{VIII}}$** lies much lower in energy than **TS′$_{\text{VIII}}$**.

The results of our DFT calculations associated with the title reaction are summarized in Scheme 6. The following points have emerged from this investigation. First, formation of aurated naphthyl cation **III** corresponds to the rate determining step, occurring with an activation barrier greater than 28 kcal/mol, explaining why such a catalytic process requires a high temperature (80 °C). Second, the mechanism for trapping aurated naphthyl cation **III** depends on the electronic nature of the employed solvent (RH). If an aliphatic solvent such as cyclohexane is utilized, then intermediate **III** interacts with the solvent C(sp^3)–H bond and immediately affords the Wheland-type species **IV** from

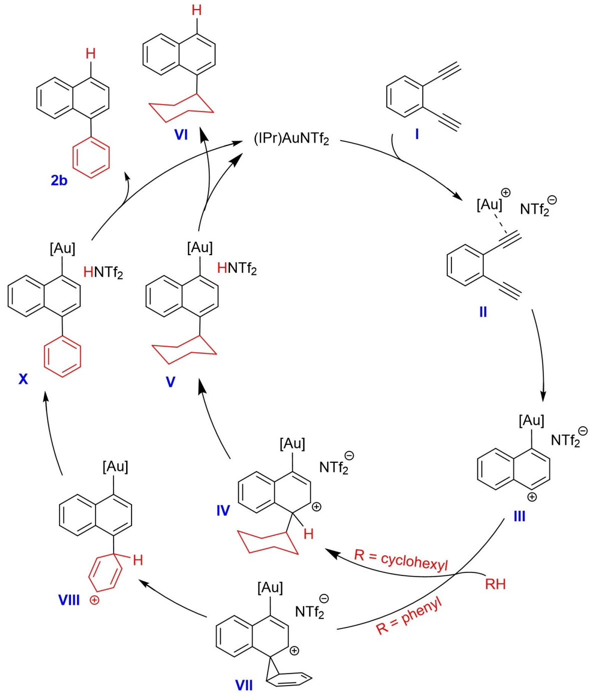

Scheme 6. Mechanism proposed according to DFT calculation.

which the deprotonation and then protodeauration steps are mediated by the $[NTf_2]^-$ counterion, producing the final product **VI** and regenerating the (IPr)AuNTf$_2$ catalyst. In contrast, if an aromatic solvent such as benzene is utilized, the π-system of the solvent does not allow aurated naphthyl cation **III** to interact effectively with the solvent C(sp^2)–H bond and thus in this case, cyclohexadienyl cation **VIII** is formed preceded by formation of phenonium ion **VII**. The ensuing cation is highly acidic and therefore is deprotonated by the $[NTf_2]^-$ counterion in a barrierless fashion, finally giving product **2b** preceded by an in situ-generated HNTf$_2$-mediated protodeauration.

Conclusion

In summary, we demonstrated that, diyne systems bearing two terminal alkyne units can also be cyclized by a pathway using a single[21] gold center. Key to unlocking this reactivity pattern was the prevention from established pathways of dual gold catalysis by the usage of a gold catalyst bearing a sterically highly demanding steering ligand. The now established mono gold 6-*endo-dig* cyclization mode results in the formation of highly reactive aryl cations, which were utilized for the intermolecular formation of C–C bonds via the insertion into aromatic as well as aliphatic C–H bonds. Thereby, from a synthetic standpoint, naphthalene scaffolds functionalized in α-position are obtained, a regioselectivity nicely complementing the typically observed β-regioselectivity of dual gold catalysis. In addition, quantum chemical calculations revealed two different mechanistic scenarios for the C–H insertion depending on the nature of the activated C–H group, namely a kinetically favored mechanism for the insertion of aromatic C–H bonds, involving the π-system of the respective aromatic hydrocarbon and a barrierless direct insertion mechanism for the insertion into aliphatic C–H bonds.

Experimental Section

General procedure for the gold-catalyzed synthesis of α-aryl- and α-alkylnaphthalene derivatives: In a crimp neck vial, 5 mol% of IPr*AuCl and 5 mol% of AgNTf$_2$ are dissolved in the respective nucleophile as solvent (100 mM with regard to the starting material) and stirred at room temperature for 10 minutes. 1.0 eq. of the diyne substrate is added, the vial is closed properly and the resulting mixture is stirred at 80 °C until complete conversion of the starting material is detected by TLC. The reaction mixture is diluted with DCM and directly evaporated onto Celite®. The crude product is purified by flash column chromatography.

Acknowledgements

J. Bucher is grateful for a Chemiefonds scholarship of the Fonds der Chemischen Industrie. The authors thank Umicore AG & Co. KG for the generous donation of gold salts.

References

[1] a) G. Dyker, *Angew. Chem. Int. Ed.* **2000**, *39*, 4237–4239; b) N. Krause, A. Hoffmann-Röder, *Org. Biomol. Chem.* **2005**, *3*, 387–391; c) A. S. K. Hashmi, *Chem. Rev.* **2007**, *107*, 3180–3211; d) A. S. K. Hashmi, M. Rudolph, *Chem. Soc. Rev.* **2008**, *37*, 1766–1775; e) Z. Li, C. Brouwer, C. He, *Chem. Rev.* **2008**, *108*, 3239–3265; f) A. Arcadi, *Chem. Rev.* **2008**, *108*, 3266–3365; g) C. H. Shen, *Tetrahedron* **2008**, *64*, 3885–3903; h) R. Skouta, C.-J. Li, *Tetrahedron* **2008**, *64*, 4917–4938; i) M. Rudolph, A. S. K. Hashmi, *Chem. Soc. Rev.* **2012**, *41*, 2448–2462; j) A. S. K. Hashmi, *Acc. Chem. Res.* **2014**, *47*, 864–876; k) L. Zhang, *Acc. Chem. Res.* **2014**, *47*, 877–888; l) H.-S. Yeom, S. Shin, *Acc. Chem. Res.* **2014**, *47*, 966–977; m) A. M. Asiri, A. S. K. Hashmi, *Chem. Soc. Rev.* **2016**, *45*, 4471–4503; n) R. Dorel, A. M. Echavarren, *Chem. Rev.* **2015**, *115*, 9028–9072; o) X. Zhao, M. Rudolph, A. S. K. Hashmi, *Chem. Commun.* **2019**, *55*, 12127–12135; p) A. Gómez-Suárez, S. P. Nolan, *Angew. Chem. Int. Ed.* **2012**, *51*, 8156–8159.

[2] a) I. Braun, A. M. Asiri, A. S. K. Hashmi, *ACS Catal.* **2013**, *3*, 1902–1907; b) X. Zhao, M. Rudolph, A. S. K. Hashmi, *Chem. Commun.* **2019**, *55*, 12127–12135.

[3] L. Ye, Y. Wang, D. H. Aue, L. Zhang, *J. Am. Chem. Soc.* **2012**, *134*, 31–34.

[4] A. S. K. Hashmi, I. Braun, M. Rudolph, F. Rominger, *Organometallics* **2012**, *31*, 644–661.

[5] A. M. Asiri, A. S. K. Hashmi, *Chem. Soc. Rev.* **2016**, *45*, 4471–4503.

[6] a) M. M. Hansmann, M. Rudolph, F. Rominger, A. S. K. Hashmi, *Angew. Chem. Int. Ed.* **2013**, *52*, 2593–2598; b) Y. Wang, A. Yepremyan, S. Ghorai, R. Todd, D. H. Aue, L. Zhang, *Angew. Chem. Int. Ed.* **2013**, *52*, 7795–7799.

[7] J. Bucher, T. Wurm, K. S. Nalivela, M. Rudolph, F. Rominger, A. S. K. Hashmi, *Angew. Chem. Int. Ed.* **2014**, *53*, 3854–3858.

[8] A. S. K. Hashmi, M. Wieteck, I. Braun, P. Nösel, L. Jongbloed, M. Rudolph, F. Rominger, *Adv. Synth. Catal.* **2012**, *354*, 555–562.

[9] a) J. Bucher, T. Wurm, S. Taschinski, E. Sachs, D. Ascough, M. Rudolph, F. Rominger, A. S. K. Hashmi, *Adv. Synth. Catal.* **2017**, *359*, 225–233; b) J. Bucher, T. Stößer, M. Rudolph, F. Rominger, A. S. K. Hashmi, *Angew. Chem. Int. Ed.* **2015**, *54*, 1666–1670.

[10] T. Wurm, J. Bucher, S. B. Duckworth, M. Rudolph, F. Rominger, A. S. K. Hashmi, *Angew. Chem. Int. Ed.* **2017**, *56*, 3364–3368.

[11] T. Wurm, J. Bucher, M. Rudolph, F. Rominger, A. S. K. Hashmi, *Adv. Synth. Catal.* **2017**, *359*, 1637–1642.

[12] H. B. Ambroz, T. J. Kemp, *Chem. Soc. Rev.* **1979**, *8*, 353–365.

[13] M. H. Larsen, K. N. Houk, A. S. K. Hashmi, *J. Am. Chem. Soc.* **2015**, *137*, 10668–10676.

[14] G. Berthon-Gelloz, M. A. Siegler, A. L. Spek, B. Tinant, J. N. H. Reek, I. E. Markó, *Dalton Trans.* **2010**, *39*, 1444–1446.

[15] B. P. Taduri, Y.-F. Ran, C.-W. Huang, R.-S. Liu, *Org. Lett.* **2006**, *8* (5), 883–886.

[16] CCDC 1977372 (**4 a**) contains the supplementary crystallographic data for this paper. These data can be obtained free of charge from The Cambridge Crystallographic Data Centre via www.ccdc.cam.ac.uk/structures.

[17] M. P. Doyle, R. Duffy, M. Ratnikov, L. Zhou, *Chem. Rev.* **2010**, *110*, 704–724.

[18] With respect to a possible resonance of the intermediate as benzene is a carbene center, we conducted a natural localized molecular orbital (NLMO) analysis (see: A. E. Reed, F. Weinhold, *J. Chem. Phys.* **1985**, *83*, 1736–1740) to examine the potential π bond interaction between Au and C1 atoms in species **III**^{c}. Based on the spatial plot derived from the NLMO calculations (Supporting Information, Scheme S3), the Au dπ orbital, with the appropriate symmetry for establishing a π interaction with the C1 atom, is calculated to be predominantly localized on the gold center with a contribution of 96.1%. Therefore, the contribution of a resonance structure involving the carbene LAu=C to the bonding of species **III**^{c} can be considered negligible.

[19] a) R. BabaAhmadi, P. Ghanbari, N. A. Rajabi, A. S. K. Hashmi, B. F. Yates, B. F. A. Ariafard, *Organometallics* **2015**, *34*, 3186–3195; b) G. Sciortino, S. Muñoz-López, A. Lledós, G. Ujaque, *Organometallics* **2020**, *39*, 3469–3479.

[20] M. Kreuzahler, S. Fabig, G. Haberhauer, R. Gleiter, *J. Org. Chem.* **2017**, *82*, 13572–13582.

[21] For early results on gold catalysis by mononuclear complexes, see: a) A. S. K. Hashmi, T. M. Frost, J. W. Bats, *J. Am. Chem. Soc.* **2000**, *122*, 11553–11554; b) A. S. K. Hashmi, L. Schwarz, J.-H. Choi, T. M. Frost, *Angew. Chem. Int. Ed. Engl.* **2000**, *39*, 2285–2288; c) A. S. K. Hashmi, T. M. Frost, J. W. Bats, *Catal. Today* **2002**, *72*, 19–27. .